Predicting Ajisai Satellite Reflected Sunlight Flashes through Modelization in the context of Time Transfer by Means of Laser Link

Author: Carlo Calatroni

Advisor: Prof. Pierluigi Di Lizia

Co-advisor: Dr. Gilles Metris

Academic year: 2022-2023

1. Introduction

Atomic clocks provide regular and stable time with incredible performances. Whether we are talking about astronomy, geodesy or telecommunications orf other scientific or commercial sectors where it is necessary to carry out comparable measurements an effective, replicable and economic time synchronization capability between two places is essential. The ability to synchronize time in two different places with an increasingly high level of accuracy is one of the main challenges that will be of great importance in reaching new frontiers in metrology.

H. Kunimori et al. [7], suggested that the timing of the laser pulses emitted by a ground station A, reflected on the Ajisai satellite surface, and received by a station B could be used to compare the clocks attached to each station.

The German Wettzell station recently demonstrated the use of space debris laser ranging, and specifically an old rocket body, for realizing time transfer at the nanosecond level via the realization of a bi-static link between two laser stations [8].

In the future, we would like to exploit the infrared laser ranging on the Ajisai satellite, combining cube corner reflectors and spherical mirrors, to demonstrate a ground-to-ground time transfer at a metrological level of the order of a few hundred picoseconds but on a passive satellite with a very high longevity.

Obtaining this metrological level requires to constrain well the attitude of the satellite to determine the surface which allowed the reflection of the pulses. To achieve this aim, the modelization of reflected sunlight flashes on the Ajisai satellite taking advantage of in-situ measurements (light curves) specifically carried out for this project by the MéO (Metrology and Optics) telescope, the Satellites and Lunar Laser Ranging dedicated telescope of Observatoire de la Côte d'Azur (France), is of major interest.

Although attempts to characterize the rotation of the satellite through photometry already exist in the literature ([3], [1], [2]), in this thesis are proposed and discussed not only various innovative tools in the analysis and direct characterization of the parameters but also the implementation of a model that simulates solar reflection with the aim of producing a light curve as similar as possible to that obtained from real observation with the prospect of exploiting the model itself for the purpose of producing attitude predictions.

Decisive novelty is added to the published state of art. First the effect of the mirrors curvature is introduced and second, comparing this complex model to the observations, the efficiency of a procedure to finely improve the determination of the rotation parameters is proved.

2. Satellite Model

In 1986, the Experimental Geodetic Satellite, EGS, named AJISAI, is launched by the National Space Development Agency of Japan, now JAXA, [9], [10].

2.1. Geometry of Mirrors and CCRs in the Body Frame

No precise data of the Ajisai satellite design and in particular no precise plan of mirrors and CCRs retroreflectors on the satellite surface is available. Our requests to the japanese space agency to get these information was unsuccesful up to now. However, starting from a figure in [3] and [2], it was possible to reconstruct a partial scheme of the mirrors in terms of nominal normal to the mirrors unit vectors (fig. 1).

Ajisai is equipped with 318 mirrors that can be subdivided in 15 rings containing between 3 and 27 mirrors. Each ring can in turn be subdivided into groups of 3 mirrors having the same inclination w.r.t. the tangent to the spherical surface of the satellite. 213 of these mirrors have been included in the mirrors model. As a results 71 triplets of mirrors having the same inclination w.r.t. the satellite axis can be identified.

2.2. Curvature of the Mirrors

The Ajisai satellite mirrors are not flat: their radius of curvature is 9 m instead of 1.075 m. Due to the extension of the mirrors in latitude, it follows that the normals to the south and to the north part of the mirror will differ by about 1.27° degrees. This is not negligible compared to the differences of inclination and should be taken into account in the reflection model.

2.3. Rotation Model

Two classical reference frames are used to describe the rotation model: the inertial ICRF frame $\mathcal{N} = \left\{ \hat{\mathbf{e}}_1^{\mathcal{N}}, \hat{\mathbf{e}}_2^{\mathcal{N}}, \hat{\mathbf{e}}_3^{\mathcal{N}} \right\}$ and the $\mathcal{B} = \left\{ \hat{\mathbf{e}}_1^{\mathcal{B}}, \hat{\mathbf{e}}_2^{\mathcal{B}}, \hat{\mathbf{e}}_3^{\mathcal{B}} \right\}$, Satellite Body Frame. The relation between the normal $\mathbf{n}_i$ expressed in $\mathcal{N}$ and
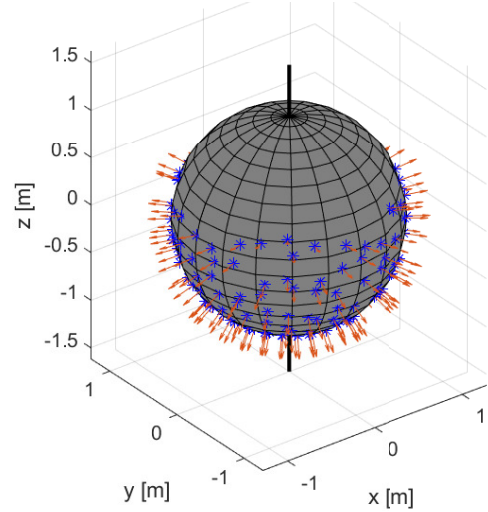

Figure 1: Ajisai mirrors direction expressed as longitude and latitude in satellite body frame where the latitude does not express the physical position but the inclination of the normal direction w.r.t. the satellite surface.

$\mathcal{B}$ reads:

$$\mathbf{n}_{\mathcal{N},i}(t) = \left[\mathbf{A}_{B/N}^T \right] \cdot \mathbf{n}_{\mathcal{B},i} \qquad (1)$$

for: $(i = 1, 2, ..., n_{mirrors})$ and $(t = t_0, ..., t_f)$.
where: $\mathbf{n}_i$ is the normal unit vector associated to mirror i and $A_{B/N}^T$ is a rotation matrix. The $A_{B/N}$ matrix can be rewritten as a sequence of the two rotation matrices:

$$\mathbf{A}_{B/N}(t) = \left(\mathbf{A}_3(\alpha) \cdot \mathbf{A}_{rod}^{\hat{\mathbf{z}} \rightarrow \hat{\mathbf{w}}}(\hat{\mathbf{u}}, \theta) \right) \qquad (2)$$

where $\mathbf{A}_3(\alpha(t))$ is the rotation matrix at instant t and

$$\mathbf{A}_3(\alpha(t)) = \begin{bmatrix} \cos(\alpha(t)) & \sin(\alpha(t)) & 0 \\ -\sin(\alpha(t)) & \cos(\alpha(t)) & 0 \\ 0 & 0 & 1 \end{bmatrix} \qquad (3)$$

$\alpha(t)$ is the phase angle in clockwise direction at instant t, t_0 is the initial time instant.
$\mathbf{A}_{rod}^{\hat{\mathbf{z}} \rightarrow \hat{\mathbf{w}}}$ corresponds to the transformation of a frame of third axis $\hat{\mathbf{z}}$ to a frame of third axis $\hat{\mathbf{w}}$ equivalent to a rotation around an axis $\hat{\mathbf{u}}$ orthogonal to $\hat{\mathbf{z}}$ and $\hat{\mathbf{w}}$ of the angle θ between the two:

$$\mathbf{A}_{rod}^{\hat{\mathbf{z}} \rightarrow \hat{\mathbf{w}}}(\hat{\mathbf{u}}, \theta) =$$
$$\cos\theta[\mathbf{I}] + (1 - \cos\theta)\hat{\mathbf{u}}\hat{\mathbf{u}}^T + \sin\theta[(\hat{\mathbf{u}})]_x \qquad (4)$$

where $[(\hat{\mathbf{u}})]_\times$ is the antisymmetric matrix constructed from the components of the unit vector $\hat{\mathbf{u}}$: u_1, u_2, u_3.

2

2.3.1 Spin Axis

The spin axis of Ajisai, $\hat{\mathbf{w}}$ can be considered collinear with its symmetry axis, the satellite body frame z'-axis pointing the north. The direction of the spin axis is changing over time. Its orientation is close to the one of the Earth but the difference is not neglectable for our use case. The difference between the z-axis of the J2000 reference frame and the spin axis direction $\hat{\mathbf{w}}$ expressed in the same frame is in the order of 1.5°, slowly but constantly growing.

The Kucharski spin axis model reported in the literature [6] expresses the motion of the spin axis through the motion of two cones describing precession and nutation respectively (fig. 2).
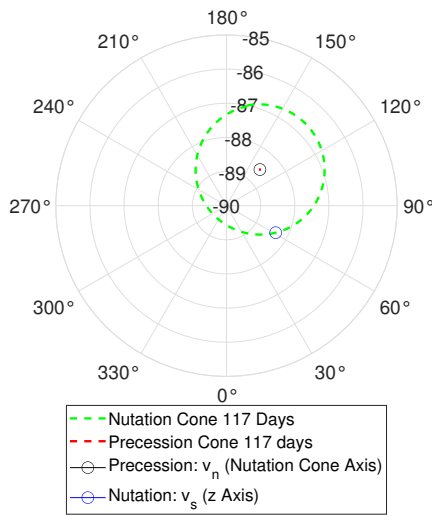

Figure 2: Ajisai Spin Axis Nutation Precession Model 24/11/2022 ±68.5 Days

2.3.2 Rotation Angle

The phase angle at the specified time instant t can be computed by using the following kinematic relationship:

$$\alpha(t) = \alpha_0 + \dot{\alpha}(t) \cdot (t - t_0) \ [rad] \qquad (5)$$

$(t = t_0, ..., t_f)$,

where: $\dot{\alpha}(t)$ is the angular velocity of the satellite at instant t, α_0 is the initial phase angle. If the initial phase angle α_0 is not know, a shift up to 1 rotation period is introduced in the model results.

2.3.3 Rotation Period

The satellite spin period changes over time; it grows following the progressive slowdown of the

rotation (angular velocity) of the satellite [4], [3], mainly caused by magnetic fields of the Earth. However, an influence can also be attributed to non-gravitational effects connected with the umbra, small perturbations of the spin period due to the solar energy flux to which the satellite is exposed and the consequent temperature distribution over the satellite body. These non-gravitational effects, are referred to as Yarkovsky-Schach effect. An estimation of the satellite rotation period $T(t)$ can be determined from an empirical relationship based on past laser observations data. Various of such formulas can be found in literature. The following formula is used in our model [3]:

$$T(t) = 1.4934 \cdot exp\left(0.000040553 \cdot (t - t_0)\right) \ [s]$$
$$(6)$$

where t_0 is the Ajisai launch date, 12/08/1986, in Modified Julian Days, 46654.

3. Sunlight Reflected Flashes Model

3.1. Flashes model overview

An optical model that permits to reconstruct the Ajisai light curve in the timescale of the station is introduced. The model simulates the solar light reflection that occurs on the Ajisai satellite mirrors with the aim of producing a light curve as similar as possible to that obtained from real observations, with, in perspective, the possibility of exploiting the model itself not only for the a posteriori analysis of the curve but also for producing a priori satellite attitude predictions.
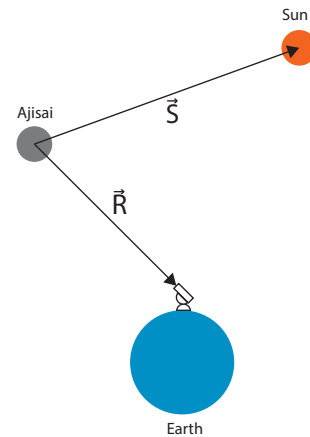

Figure 3: Earth - Sun - Satellite Model Scheme of Ajisai Sunlight Reflected Flashes Model.

The elements that constitute the model (fig. 3) are:

- $\hat{\mathbf{S}}$ Satellite - Sun Direction
- $\hat{\mathbf{R}}$ Satellite - Station (Telescope) Direction
- $\hat{\mathbf{n}}_i$ i−th Mirror Normal Unit Vector

3.2. Optical model

3.2.1 General principle

Given the normal $\hat{\mathbf{n}}_i$ to the mirror M_i, we define the symmetric $\hat{\mathbf{R}}'$ of $\hat{\mathbf{R}}$ w.r.t. $\hat{\mathbf{R}}$:

$$\hat{\mathbf{R}}' = 2\left(\hat{\mathbf{R}} \cdot \hat{\mathbf{n}}\right)\hat{\mathbf{n}} - \hat{\mathbf{R}} \qquad (7)$$

In the case of a point-like Sun of direction $\hat{\mathbf{S}}$, the condition to have a reflection from $\hat{\mathbf{S}}$ toward $\hat{\mathbf{R}}$ (or eqivalently from $\hat{\mathbf{R}}$ to $\hat{\mathbf{S}}$) is that

$$\hat{\mathbf{R}}' \equiv \hat{\mathbf{S}} \qquad (8)$$

The Sun cannot be considered as a material point but rather as a disk of apparent radius (or angular radius) ε. The flash condition shall be updated accordingly:

$$\Rightarrow \angle\left(\hat{\mathbf{R}}', \hat{\mathbf{S}}\right) \leq \varepsilon \Rightarrow \hat{\mathbf{R}}' \cdot \hat{\mathbf{S}} \geq \cos(\varepsilon)$$

3.2.2 Curvature of the mirrors

The Ajisai satellite mirrors are not flat as assumed up to now in our discussion about light reflection but they have a $9\ m$ curvature radius. This means that the mirrors have no longer a unique normal but their normal depends of the position on the mirror. Deriving a generalized flash condition for this case seems out of reach. For this reason, we have used a discretized model. In order to represent the curvature of a mirror in the model satellite body frame, the mirror surface is discretized by using a set of unit vectors normal to the surface evenly distributed over the surface itself. The nominal mirror normal unit vector, in the center of the mirror, is used as the reference for the discretization.

The flash condition needs to be formally updated in order to account for the discretization introduced above.

$$\begin{cases} 2\left(\hat{\mathbf{R}} \cdot \hat{\mathbf{n}}_{i,j}\right)\left(\hat{\mathbf{S}} \cdot \hat{\mathbf{n}}_{i,j}\right) \geq \left(\hat{\mathbf{R}} \cdot \hat{\mathbf{S}}\right) \\ \qquad\qquad\qquad\qquad + \cos(\varepsilon) \\ \left(\hat{\mathbf{R}} \cdot \hat{\mathbf{n}}_{i,j}\right) > 0 \end{cases} \qquad (9)$$
$$(i = 1, \cdots, N_{mirrors}; \quad j = 1, \cdots, N_{disc})$$

where $N_{mirrors}$ is the number of mirrors, N_{disc} is the number of discretized normals, $\mathbf{n}_{i,j}$ is the j−th discretized normal unit vector associated to the i−th mirror.

3.3. Typical results and the importance of the curvature

As it can be noted in fig. 4, the introduction of the curvature of the mirrors allows to drastically increase the coherence of the simulated curve with the one observed with respect to the approximation with flat mirrors. However, this involves a higher computational cost.

4. Observations

4.1. Observational Process and Available Data

Two experiments were performed using two different observation techniques with a relatively different hardware configuration. In the first experiment, a τ-SPAD system, Single Photon Avalanche Diode, (Trigger or Geiger Mode) is used, while in the second one a linear detector, Avalanche Photo Diodes in Linear amplifying mode is used.

4.1.1 The MéO Station

The MéO (Metrology and Optics) station, generally known as "Grasse Station" was initially designed in the framework of a laser ranging program dedicated to the moon. It subsequently enlarged its scientific objectives to laser links in general and it participates now to the ILRS network and various other research activities. The station is based on a 1.54 meter Ritchey Chretien telescope installed on an Alt-Az mount.

4.1.2 Experiment 1 - Single Photon Counting

Thanks to a control by a computer, the telescope follows the direction of the moving target. The entire flux received by the telescope is sent to the single-photon detector (SPAD Single-Photon Avalanche Diode). The detector is in free-running mode, meaning that when it is triggered by a photon, the electrical signal resulting from the absorption of the photon on the active silicon zone is stopped.
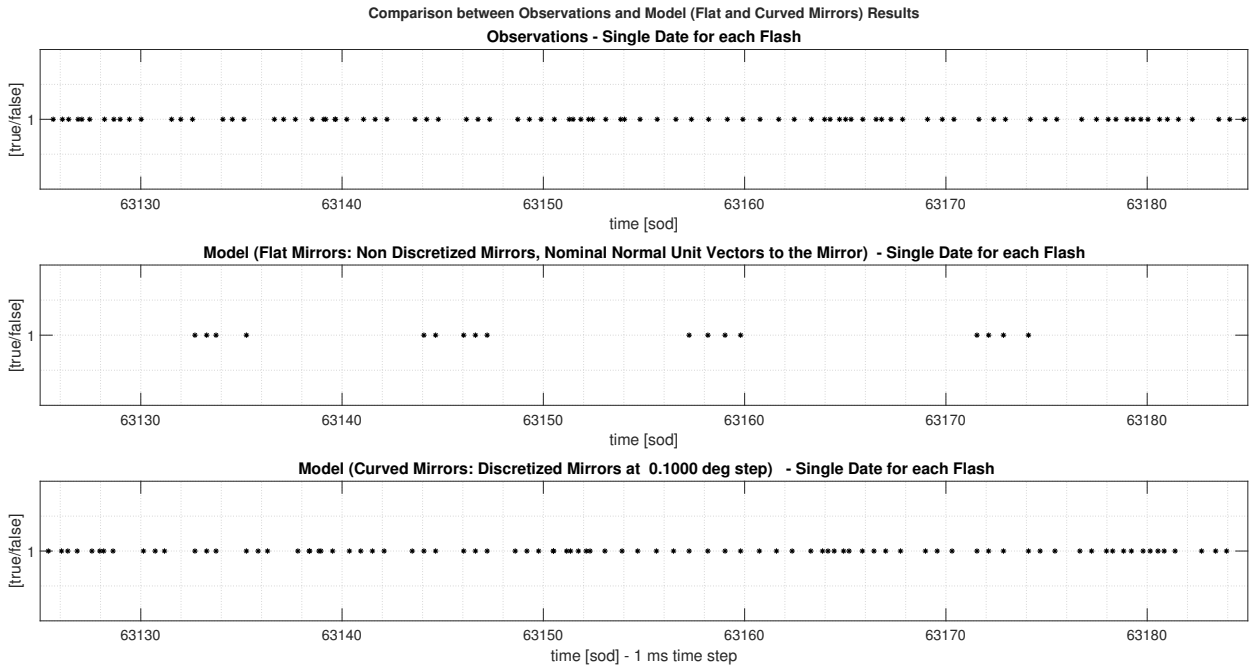
Figure 4: Comparison of observations identified flashes, model simulated flashes using flat and curve mirrors. (Observations: 24/11/2022_1)

The electrical signal from the avalanche has been splitted in two and simultaneously sent to the SR620 counter and a SigmaWorks STX picosecond timer. The latter instrument is capable of absolutely dating the time of arrival of the photons in the local time scale. However, this timer proved to be limited for our experiments because of saturation during the Ajisai flashes, and the timer was unable to date too many data over a short period of time (10 kCounts max continuously) with sub-picosecond resolution.

4.1.3 Experiment 2 - Linear Photometry

In Experiment 2, a different set of instruments has been used. The telescope follows the passage predictions. A detector to provide a linear measurement of the received photon flux has been used (fig. 5). The detector's electrical output signal is sent to a digitiser, which samples the signal at 5k samples/s. The entire acquisition chain has a bandwidth of 2 kHz, which is more compatible with Ajisai's flash duration (which is about 10 ms).

4.1.4 Available Observations

The data used in this thesis consists of the observations of several passes of the satellite with different equipment settings in both day and night conditions. A total of 13 Ajisai satellite passes have been observed and data collected: 8 passes using τ-SPAD and 5 using linear photometry. 2 and 3 of these were respectively selected to be preprocessed and analyzed.

4.2. Preprocessing of Observations and model outputs

Raw observations data, obtained in experiment 1, give us dates of photons that trigger the single pixel detector while those obtained in experiment 2 give us linearly detected light flux measurments at equispaced time instants. In order to make useful use of this data, they need to be preprocessed.

4.2.1 Identify Flash Condition

In no-flash condition the photons are relatively largely spaced in time. During a flash, the photons time rate grows rapidly and remains high until the end of the flash. This translates mathematically to determine when the filtered derivative of photon dates approaches to zero, i.e. it is lower than a sufficiently low threshold. The results obtained are integrated on an equally spaced set of time instants.
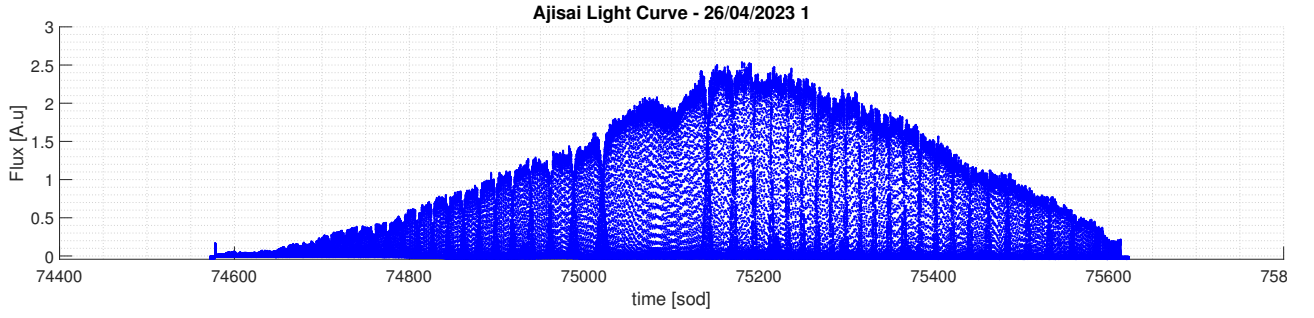A procedure has been introduced to filter (mov-

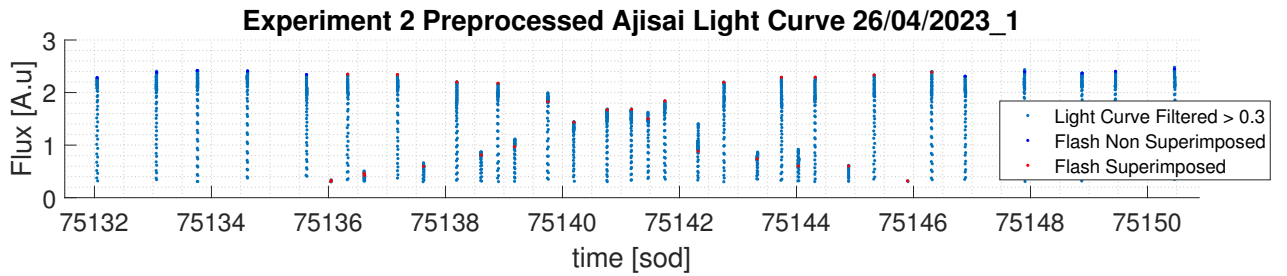Figure 5: Experiment 2 Linear Photometry Light Curve Example

Figure 6: Experiment 2 Linear Photometry Light Curve Example

ing average), derive (pseudo forward differences), select (a threshold $\delta t^{it}_{filtered} \leq 10^{-5}$) and integrate photon dates that constitutes flashes. Following this procedure, not only the flash condition for each instant of time is determined but also the intensity information is at least partially preserved.

The different steps are the followings:
1. Filtering High Frequency
2. Pseudoderivation of Photons Dates
3. Extract/Select Flashes Photons Dates
4. Integration using a Regular Step Time Span

4.2.2 Single Date for each Flash

The flash condition can be expressed as a boolean condition true/false for each time instant or equivalently as a discrete sequence of dates in which the flash condition is verified. In order to express each flash using a single date, it is necessary to further process the observations to delimit which flashes date belong to the same flash. The midpoint of the flash in terms of time duration is used as the reference date and only this date is mantained in the processed light curve.

4.2.3 Remove Superimposed Time Frame Flashes From Observations

As expected from modelization (section 3.3), the curvature of the mirrors leads to some sequences during which 2 triplets of mirrors are simultaneously flashing during the same rotation period. Flashes that are included in a time span where there is a superimposition of flashing triplets need to be discarded. For this reason, for each flash date (derivative), we need to determine if it's part of a period where no more and no less than three flashes have been detected.

$$\delta t^k = t^k - t^{k-1} \qquad (k = 2, \cdots, n) \qquad (10)$$

For each flash f_k, a "test period" is computed by summing 3 neighbour δt, determined using pseudobackward differences of single flash dates (eq. (10)), and it is verified if the difference with the predicted value is smaller than a threshold δT: $T_{predicted} - \delta T \leq T_{test} \leq T_{predicted} + \delta T$.

5. Matching Model and Observations

5.1. Triplets and Mirrors Identification in the Observations

The driving idea of the identification of the flashing mirrors is that each $i-$th mirrors triplet

$\mathbf{MT}_i \supset [m_{i,1}, m_{i,2}, m_{i,3}]$ is differently distributed in longitude $\underline{\lambda}_{\mathbf{MT}_i} = [\lambda_{l1}, \lambda_{l2}, \lambda_{l3}]$ and can be characterized by the differences of longitude between the mirrors:

$$\underline{\Delta\lambda}_i = [\Delta\lambda_{i,l1-l2}, \Delta\lambda_{i,l2-l3}, \Delta\lambda_{i,l3-l1}] \\ = [\Delta\lambda_{i,1}, \Delta\lambda_{i,2}, \Delta\lambda_{i,3}] \quad (11)$$

where $(l1, l2, l3)$,order of the sequence of mirrors is equal to $(1, 2, 3)$ in the clockwise and $(3, 2, 1)$ in the counterclockwise rotation direction of the spacecraft.
Knowing the rotation period T of the satellite, these differences of longitude can be associated to differences of time:

$$\underline{\Delta t}_i = [\Delta t_{i,1}, \Delta t_{i,2}, \Delta t_{i,3}] \quad (12)$$

using the relation:

$$\Delta t_{i,j} = \frac{\Delta\lambda_{i,j} * T}{360} \quad [s] \quad (13)$$

for $i = 1, \cdots, N_{\mathbf{MT}}$ and $j = 1, 2, 3$.
A pseudo-forward derivative of flashes dates $\mathbf{t_{f^*_{obs}}}$ can be used to obtain a sequence of intervals of time associated to the series of observed flash and in turn a series of flashes triplets $\mathbf{FT}_k \supset [f_{k,1}, f_{k,2}, f_{k,3}]$ associated to a sequence of 3 intervals of time: $\underline{\Delta\tau}_k = [\Delta\tau_{k,1}, \Delta\tau_{k,2}, \Delta\tau_{k,3}]$
The next step is to associate the sequence $\underline{\Delta\tau}_k$, derived from observations, to the associated Δt_i, computed from the model.
The principle is to compare each sequence $\underline{\Delta\tau}_k$ to all sequence $\underline{\Delta t}_i$ to find the closest. To reach this result the residual:

$$r_{k,i}^{(p)} = \sum \|\underline{\Delta\tau}_k - \underline{\Delta t_i}\| \quad (14)$$

where $p \in \{1, 2, 3\}$.

$$r_k^{(min)} = min\left(r_{k,i}^{(min)}\right), \\ i = (1, \cdots, N_{\mathbf{MT}}) \quad (15)$$

is selected for $k = (1, \cdots, N_{\mathbf{FT}})$. Finally, mirrors triplet $\mathbf{MT}_i$ matching $\mathbf{FT}_k$ is recovered from the i_{min} index while the sequence, according to which the mirrors flashed, can be recovered from the permutation index p_{min}.

5.2. Determination of Rotation Parameters Directly from Observations

5.2.1 Period Estimation

Two methods have been tested for rotation period estimation: a statistical approach, autocorrelation and the newly developed "4-Flashes Method".

Autocorrelation The difference between predicted (eq. (6)) and computed values of the apparent period is equal to 2 ms for experiment 1 data and between 2 and 4ms for experiment 2 data.

4 Flashes Method If we consider that in each period only three flashes occur, it is clear that it is sufficient to know the dates of 4 successive flashes belonging to the same triplet (ie having the same latitude in the body frame) to obtain the apparent rotation period of the satellite.
If k_1, k_2, k_3 and k_4 are the four indexes of the flashes, the period T can be easily computed as:

$$T = t(k_4) - t(k_1) \quad (16)$$

There is a substantial consistency between the values of the apparent period determined through autocorrelation and the values deriving from the average of the periods calculated during the satellite pass through the 4 flashes method.

Aberrations Two main aberrations should be considered: a first linked to the speed of propagation of light and a second of a geometric type due to the contemporary and relative movement of the satellite, station and Earth.

5.2.2 Determination of the Spin Axis Directly from Observations

A first research method of the spin axis is proposed starting from observations alone and it is inspired by what proposed in [1] and later in [3], with the necessary adjustments.
The principle is that a flash emitted by the Sun in the direction $\hat{\mathbf{S}}$ toward the telescope in the direction $\hat{\mathbf{R}}$ must result from a reflexion on a piece of mirror having a normal parallel to the bisector $\hat{\mathbf{B}}$. Thus, in a first approximation, the

normal $\hat{\mathbf{N}}$ of the identified mirror should correspond to $\hat{\mathbf{B}} = \dfrac{\mathbf{R}+\mathbf{S}}{\|\mathbf{R}+\mathbf{S}\|}$; in particular they must have the same latitude (or equivalently the same colatitude) w.r.t. the spin axis. The colatitude of the identified normal $\hat{\mathbf{N}}$ is fixed by the satellite design while the colatitude β of $\hat{\mathbf{B}}$ depends on the orientation of the spin axis.

Thus, the potential discrepancy between β and ϕ can be interpreted as a misorientation of the spin axis. That is why the objective will be to search for the spin axis orientation which minimize the discrepancy.

Objective Function

$$F = \sum \left(\| \phi - \beta \left(\alpha_{pol}, \delta_{pol} \right) \| \right) \qquad (17)$$

Statement of the Problem

$$\min_{\alpha_{pol}, \delta_{pol}} \quad F \rightarrow \begin{cases} 0° \leq \alpha_{pol} \leq 360° \\ 85° \leq \delta_{pol} \leq 90° \end{cases} \qquad (18)$$

The method allows to compute a quite accurate estimation of the spin axis in limited cpu-time.

5.3. Determination of Rotation Parameters from Model and Observations Comparison

A method to determine or increase the accuracy of the rotation parameters, specifically the spin axis, and to find the rotation angle, based on an a posteriori comparison between the light curves observed determined starting and the one reproduced by the model has been developed. The spin axis is determined from an iterative matching of the preprocessed light curve obtained from observations with a light curve (intended here as a sequence flashes dates) generated by the model using an imposed spin axis iteratively extracted from a search grid (fig. 7). A possible objective function is defined as follows:

$$L_1 = \sqrt{\frac{1}{N_{lat}} \cdot \sum_{i=1}^{N_{lat}} \left(t_i^{observations} - t_i^{model} \right)^2} \quad (19)$$

where N_{lat} is the number of different groups of flashes with the same latitude in which flashes are registered.

When the values of L_1 have been computed for all tested spin axis, we look for the minimum of L_1.
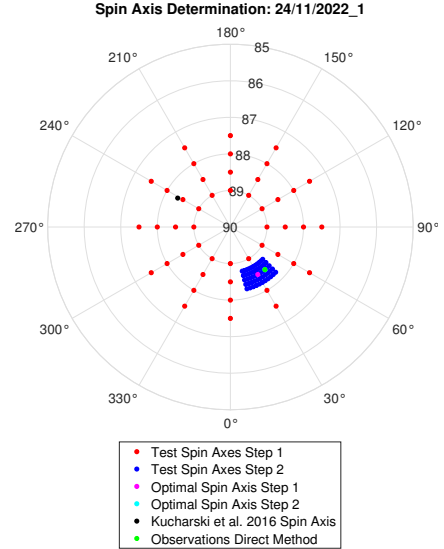

Figure 7: Determination of the Spin Axis from Model and Observations Matching.

Figure 8 shows the coherence of the observed and the simulated flashes curves comparing the determined optimal (fig. 8a) w.r.t. the predicted [6] (fig. 8b) spin axis.

5.3.1 Rotation Angle Estimation

The rotation angle, or phase angle, of Ajisai can be determined using satellite laser ranging [5]. However, It would be of great interest to be able to determine also the phase additionally to the period and the spin axis with photometry alone. The proposed approaches envisage the iterative simulation of a portion or an entire passage of the satellite through the model in order to produce a flash curve that can be compared with the observed one according to the same principle used for the spin axis. If it is possible to associate a flash in the observations to the corresponding flash in the model, the initial phase angle can be computed from the Δt between the two flashes dates knowing that the model flash date is computed imposing $\alpha_0 = 0$.

6. Conclusions and Future Developments

Various interesting results emerged. Satellite rotation have been characterized through high frequency photometry and its main parameters have been directly estimated from observations. A scheme of the mirrors and retroreflectors (CCRs) position and specifically inclinations

(a) Model using [6] spin axis
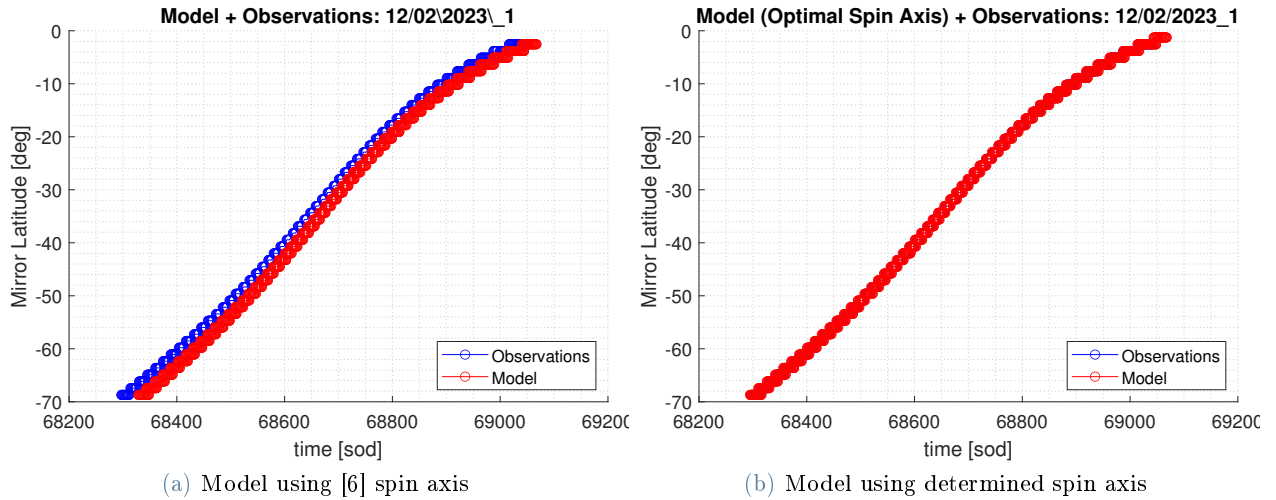
(b) Model using determined spin axis

Figure 8: Light Curves Comparison before and after the spin axis determination.

w.r.t. the surface have been reconstructed from satellite specifications and literature data. The mirrors rotation as a function of time has been modelized using empirical relationships derived from laser ranging and available in literature.

A crucial element of novelty has therefore been introduced with respect to previous studies available in literature. A model which reproduces with high fidelity the sequence of flashes "referred to as "light curve" due to the reflection of the Sun light on the Ajisai satellite mirrors have been introduced. The model simulates the curve as a function of the rotation spin axis, the rotation angle around the spin pole and the rotation period.

The rotation spin period and the spin axis have been determined directly from single pass observations. The model has been used to retrieve rotation parameters, specifically the spin axis, through an iterative differential comparison against the observations.

The model and methods developed in this thesis allow not only to classify the flashes and extract the rotation parameters of the satellite thanks to the use of photometry alone (without satellite laser ranging support) but also to reproduce, given the rotation parameters, the flash curve itself with a good degree of fidelity.

In perspective, there is the possibility of exploiting the model itself not only for the a posteriori analysis of the curve but also for producing a priori satellite attitude predictions. The a priori characterization of the parameters in the form of predictions might enable the real time determination of the main rotation parameters, during future passes of the satellite.

The use of photometry in real time and all together with the use of lasers, during the time transfer, from one or both stations involved simultaneously, would allow to characterize the rotation of the satellite during the pass of the satellite, making it possible to synchronize the activation of the laser with the rotation of the mirrors disengaging from the need to use ultra-high repetition rate laser systems. This would enable the choice of target mirror and firing times according to the satellite orbit and attitude.

Starting from the studies carried out on the rotation, by analyzing a larger number of observations, in conjunction with the available SLR observations, a model of the dynamics of the Ajisai rotation could be developed.

7. Acknowledgements

References

[1] N. Burlak, N. Koshkin, E. Korobeynikova, S. Melikyants, L. Shakun, and S. Strakhova. The Research of Variation of the Period and Precession of the Rotation Axis of EGS (AJISAI) Satellite by Using Photometric Measurement. *Odessa Astronomical Publications*, 27:83, January 2014. ADS Bibcode: 2014OAP....27...83B.

[2] E. Korobeynikova, N. Koshkin, S. Shakun, N. Burlak, S. Melikyants, S. Terpan, and S. Strakhova. The Photometric Model of Artificial Satellite Ajisai and Determination of its Rotation Period. *Odessa Astronomical Publications*, 25:216, January 2012. ADS Bibcode: 2012OAP....25..216K.

[3] N. Koshkin, L. Shakun, N. Burlak, E. Korobeynikova, S. Strakhova, S. Melikyants, S. Terpan, and A. Ryabov. Ajisai spin-axis precession and rotation-period variations from photometric observations. *Advances in Space Research*, 60(7):1389–1399, October 2017.

[4] D. Kucharski, G. Kirchner, T. Otsubo, and F. Koidl. 22Years of AJISAI spin period determination from standard SLR and kHz SLR data. *Advances in Space Research*, 44(5):621–626, September 2009.

[5] D. Kucharski, G. Kirchner, T. Otsubo, and F. Koidl. The Impact of Solar Irradiance on AJISAI's Spin Period Measured by the Graz 2-kHz SLR System. *IEEE Transactions on Geoscience and Remote Sensing*, 48(3):1629–1633, March 2010.

[6] Daniel Kucharski, Georg Kirchner, Toshimichi Otsubo, Hyung-Chul Lim, James Bennett, Franz Koidl, Young-Rok Kim, and Joo-Yeon Hwang. Confirmation of gravitationally induced attitude drift of spinning satellite Ajisai with Graz high repetition rate SLR data. *Advances in Space Research*, 57(4):983–990, February 2016.

[7] Hiroo Kunimori, Fujinobu Takahashi, Toshikazu Itabe, and Atsushi Yamamoto. Laser ranging application to time transfer using geodetic satellite and to other Japanese space programs. In *NASA. Goddard Space Flight Center, Eighth International Workshop on Laser Ranging Instrumentation*, June 1993. NTRS Author Affiliations: Ministry of Posts and Telecommunications, Maritime Safety Agency NTRS Document ID: 19940011082 NTRS Research Center: Legacy CDMS (CDMS).

[8] T. Liu, J. J. Eckl, M. Steindorfer, P. Wang, and K. U. Schreiber. Accurate ground-to-ground laser time transfer by diffuse reflections from tumbling space debris objects. *Metrologia*, 58(2):025009, March 2021. Publisher: IOP Publishing.

[9] Minoru Sasaki. Japanese Geodetic Satellite for Expansion of Marine Control. In *Proceedings International Symposium on Marine Positioning*, pages 77–85. Springer Netherlands, Dordrecht, 1987.

[10] Minoru Sasaki and Hidekazu Hashimoto. Launch and Observation Program of the Experimental Geodetic Satellite of Japan. *IEEE Transactions on Geoscience and Remote Sensing*, GE-25(5):526–533, September 1987.